Int. J. Heat Mass Transfer. Vol. 25, No. 7, pp. 925–934, 1982.
Printed in Great Britain

0017-9310/82/070925-10 $03.00/0
Pergamon Press Ltd.

NATURAL CONVECTION ADJACENT TO A VERTICAL ISOTHERMAL HOT PLATE WITH A HIGH SURFACE-TO-AMBIENT TEMPERATURE DIFFERENCE

L. R. CAIRNIE and A. J. HARRISON
Shell Research Ltd., Thornton Research Centre, P.O. Box 1, Chester CH1 3SH, U.K.

(*Received* 6 *February* 1982 *and in revised form* 8 *October* 1981)

Abstract—The free convection boundary layer flow adjacent to a vertical isothermal hot plate with high surface-to-ambient temperature difference has been investigated experimentally and theoretically. Experimental measurements of the temperature and velocity fields for plate temperatures up to 698 K have been made using the techniques of fine wire thermocouple thermometry and real fringe laser Doppler anemometry, respectively. The experimental results deviate progressively from Ostrach's solution as the plate temperature is increased. A numerical solution of the boundary layer equations which includes the temperature dependence of the fluid properties, including density, has been obtained using a finite difference scheme. Very good agreement between the numerical solution and the experimental measurements was obtained. Calculations using the Chapman–Rubesin approximation have shown that this method gives an adequate representation of the flow for many purposes.

NOMENCLATURE

C_p, specific heat at constant pressure;

f, $= \frac{1}{4\nu_r}\left(\frac{g\Delta T}{4T_\infty \nu_r^2}\right)^{-1/4} x^{-3/4}\psi$, non-dimensional stream function;

g, gravitational acceleration;

g_L, g_R, finite difference form of boundary conditions [equation (21)];

Gr_x, $= \frac{g\Delta T x^3}{T_\infty \nu_r^2}$, local Grashof number;

k, thermal conductivity;

$L(\theta)$, $= \frac{1}{Pr_r}\cdot\frac{C_p}{C_{p_r}}\cdot\frac{\rho k}{\rho_r k_r}$, fluid property combination;

$M(\theta)$, $= \frac{\rho\mu}{\rho_r\mu_r}$, fluid property combination;

$\dot{M}(\theta)$, $= \frac{d}{d\theta}\left(\frac{\rho\mu}{\rho_r\mu_r}\right)$, fluid property combination;

Nu_x, local Nusselt number;

Pr, $= C_p\mu/k$, Prandtl number;

s, $= \frac{df}{d\eta}$, function in 1st-order formulation;

t, $= \frac{ds}{d\eta}$, function in 1st-order formulation;

T, absolute fluid temperature;

T_f $= (T_w + T_\infty)/2$, film temperature;

ΔT, $= T_w - T_\infty$, plate-to-ambient temperature difference;

u, velocity component in x-direction;

v, velocity component in y-direction;

w, $w^T = (f, s, t, \theta, \phi)$, vector of variables;

x, coordinate along plate, measured upwards from leading edge;

y, coordinate normal to plate;

$Y(\theta)$, $= \frac{1}{Pr_r}\cdot\frac{C_{p_r}}{C_p}\cdot\frac{d}{d\theta}\left(\frac{\rho k}{\rho_r k_r}\right)$, fluid property combination.

Greek symbols

η, $= \left(\frac{g\Delta T}{4T_\infty \nu_r^2}\right)^{1/4} x^{-1/4}\int_0^y \left(\frac{\rho}{\rho_r}\right)dy$, independent variable;

η_O, $= \left(\frac{g\Delta T}{4T_\infty \nu_r^2}\right)^{1/4} x^{-1/4} y$, similarity variable for Ostrach's solution;

θ, $= (T - T_\infty)/\Delta T$, dimensionless temperature;

μ, dynamic viscosity;

ν, kinematic viscosity;

ξ, $= x$, independent variable;

ρ, density;

ϕ, $= d\theta/d\eta$, function in 1st-order formulation;

ψ, compressible stream function.

Subscripts

∞, ambient conditions;

r, fixed reference conditions;

w, conditions at wall;

i, mesh point in finite difference formulation;

N, maximum value of i.

1. INTRODUCTION

THIS PAPER describes a theoretical model and experimental results characterising the natural convection of air, at 1 atm pressure, induced by very hot vertical surfaces. It represents the first stage in a programme aimed at quantifying conditions critical to autoignition of hydrocarbon/air mixtures by hot surfaces for configurations of practical importance.

Several factors influence the critical surface temperature required for the autoignition of fuel/air mixtures. One of the most important of these, but the least well understood, is the convective transport in the region of the hot surface. In almost all cases of practical interest, the existence of natural convection induced by the hot surface means that the surface temperatures required before autoignition poses a hazard are much higher than those needed to ignite a similar fuel/air mixture in a quiescent system. In order to be able to make realistic appraisals of the hazard we have embarked upon a detailed investigation of the influence of natural convection on the hot-surface autoignition phenomenon.

We have selected for initial study the laminar free convective boundary layer adjacent to a vertical isothermal flat plate. This system has the advantage that the flow is fairly simple and has been the subject of many theoretical and experimental investigations. We bear in mind throughout our experimental and theoretical approach, however, that our next stage will be to consider the case of a reacting flow.

The first exact solution of the laminar boundary layer equations for the flat plate problem was obtained by [1]. Comparison of his computed temperature and velocity profiles with the experimental results of [2] showed fairly good agreement. Ostrach's [1] solution, however, relies on simplifying the boundary layer equations by the Boussinesq approximation, where the fluid is incompressible except in the buoyancy force, and by assuming constant thermal properties. The validity of these approximations is limited to small plate-to-ambient temperature differences. For large temperature differences (e.g. $\Delta T > 200\,\mathrm{K}$), conditions typical of autoignition systems, it is necessary to consider the temperature dependence of the fluid properties, including density. Sparrow and Gregg [3] were the first to investigate the variable fluid property problem in detail. They used a Howarth–Dorodnitsyn transformation on the coordinate normal to the plate to describe the density variations in this direction and tried several different functions to represent the temperature dependence of the thermal conductivity and viscosity. From their calculations they derived a set of correlations for some of the flow properties of engineering interest, for example the heat transfer at the wall. These correlations were obtained from the Ostrach solution by evaluating the fluid properties at a reference temperature. Clarke [4] retained the Howarth–Dorodnitsyn transformation used by [3] but used the Chapman–Rubesin approximation (i.e. choosing a constant representative value of the product viscosity × density). There is little published data with which to test the validity of the results obtained by these different approaches under conditions where the fluid property variations make a significant difference to the flow.

Our investigation of the autoignition phenomenon has required a detailed study of the variable property problem to define the boundary layer flow under typical autoignition conditions in the absence of chemical reaction. Accordingly, our preliminary investigation, reported here, has been to characterise the temperature and velocity fields of the non-reacting free convection boundary layer flow adjacent to very hot surfaces. We have solved the boundary layer equations without making the Boussinesq or constant property approximations and have made experimental measurements for comparison with the model.

2. THEORETICAL MODELLING

2.1. *Equations of motion and analysis*

We consider the steady, laminar, 2-dim. boundary layer flow of a fluid adjacent to a heated vertical plate. The fluid is compressible, with variable thermal properties, and the buoyancy term in the momentum equation is in the form applicable to an ideal gas. For air, the pressure work and viscous dissipation are negligible in laboratory-scale flows.

The 1st-order boundary layer approximation is applied to the equations of motion, and a compressible stream function formulation is introduced. Following [3] the equations are transformed into "similarity" form, using a Howarth–Dorodnitsyn type of variable η compared with the constant property similarity variable η_0. The resulting momentum and energy equations are

$$\frac{\partial}{\partial\eta}\left(\frac{\rho\mu}{\rho_r\mu_r}\frac{\partial^2 f}{\partial\eta^2}\right)+3f\frac{\partial^2 f}{\partial\eta^2}-2\left(\frac{\partial f}{\partial\eta}\right)+\theta = 4\xi\left(\frac{\partial f}{\partial\eta}\frac{\partial^2 f}{\partial\eta\,\partial\xi}-\frac{\partial f}{\partial\xi}\frac{\partial^2 f}{\partial\eta^2}\right) \quad (1)$$

$$\frac{\partial}{\partial\eta}\left(\frac{\rho k}{\rho_r k_r}\frac{\partial\theta}{\partial\eta}\right)+3Pr_r\left(\frac{C_p}{C_{p_r}}\right)f\frac{\partial\theta}{\partial\eta} = 4\xi\,Pr_r\left(\frac{C_p}{C_{p_r}}\right)\left(\frac{\partial f}{\partial\eta}\frac{\partial\theta}{\partial\xi}-\frac{\partial f}{\partial\xi}\frac{\partial\theta}{\partial\eta}\right) \quad (2)$$

with boundary conditions

$$f(\xi,0)=\frac{\partial f}{\partial\eta}(\xi,0)=0, \quad (3a)$$

$$\frac{\partial f}{\partial\eta}(\xi,\infty)=0, \quad (3b)$$

$$\theta(\xi,0)=1;\quad \theta(\xi,\infty)=0. \quad (3c)$$

We note that the isothermal boundary conditions in equation (3c) allow a similarity solution to equations (1) and (2), in which f and θ are functions of η alone; the equations become ordinary differential equations, with the ξ-dependent terms zero. This similarity solution is the extension of Ostrach's constant property solution to compressible, variable property flow.

For autoignition flows with chemical reaction, the presence of a heat release term in the energy equation (2) will lead to explicit ξ-dependence of the variables θ and f. Similarity solutions are therefore only possible in the absence of chemical reactions.

2.2. *Numerical solution*

For non-reacting flow, the similarity solution is determined by the stationary 2-point boundary value problem obtained by setting the right-hand sides of equations (1) and (2) to zero. These equations are then 3rd-order in f and 2nd-order in θ; however it is not only the primary variables f and θ that are of physical interest. The streamwise velocity, u, is related to $\mathrm{d}f/\mathrm{d}\eta$, the shear stress to $\mathrm{d}^2f/\mathrm{d}\eta^2$, and the heat transfer to $\mathrm{d}\theta/\mathrm{d}\eta$. It is advantageous to solve the equations as a set of five 1st-order equations, so that the derivative quantities are solved for directly, and to the same order of accuracy as the primary variables. This procedure also has the advantage of simplicity in formulation and implementation.

The temperature dependence of the fluid properties in equations (1) and (2) are incorporated in the following functions:

$$M(\theta) \equiv \frac{\rho\mu}{\rho_r\mu_r}; \quad \dot{M}(\theta) = \frac{\mathrm{d}M}{\mathrm{d}\theta} \tag{4}$$

$$L(\theta) \equiv \frac{1}{Pr_r}\left(\frac{C_{p_r}}{C_p}\right)\frac{\rho k}{\rho_r k_r};$$

$$Y(\theta) = \frac{1}{Pr_r}\left(\frac{C_{p_r}}{C_p}\right)\frac{\mathrm{d}}{\mathrm{d}\theta}\left(\frac{\rho k}{\rho_r k_r}\right). \tag{5}$$

For numerical calculations, data for the properties ρ, μ, k and C_p have been taken from [5], and interpolated as functions of temperature using cubic splines. The Chapman–Rubesin approximation may be obtained by setting M and L to constants with $L = M/Pr$ and $\dot{M} = Y = 0$. The resulting equations can be related to the Ostrach equations ($M = 1$) by the transformations $\eta' = M^{-1/2}\eta$, $F = M^{-1/2}f$; the definition of η' however is different from the Ostrach similarity variable η_O both because of the factor $M^{-1/2}$ and because of the Howarth–Dorodnitsyn definition of η.

Introducing functions $s(\eta)$, $t(\eta)$ and $\theta(\eta)$, the 1st-order formulation of the full variable property equations becomes

$$\left.\begin{aligned} \frac{\mathrm{d}f}{\mathrm{d}\eta} &= s \\ \frac{\mathrm{d}s}{\mathrm{d}\eta} &= t \\ M(\theta)\frac{\mathrm{d}t}{\mathrm{d}\eta} &= -\dot{M}(\theta)\phi t - 3ft + 2s^2 - \theta \\ \frac{\mathrm{d}\theta}{\mathrm{d}\eta} &= \phi \\ L(\theta)\frac{\mathrm{d}\phi}{\mathrm{d}\eta} &= -Y(\theta)\phi^2 - 3f\phi \end{aligned}\right\} \tag{6}$$

with separated boundary conditions

$$\left.\begin{aligned} \eta = 0: \quad f(0) &= 0 \\ s(0) &= 0 \\ \theta(0) &= 1 \end{aligned}\right\}; \quad \left.\begin{aligned} \eta = \infty: \quad s(\infty) &= 0 \\ \theta(\infty) &= 0 \end{aligned}\right\} \tag{7}$$

Equations (6) may be written together in vector form as

$$\frac{\mathrm{d}w}{\mathrm{d}\eta} = F(w) \tag{8}$$

where $w^T = (f, s, t, \theta, \phi)$. The boundary conditions are of the form

$$\left.\begin{aligned} g_L[w(0)] &= 0 \\ g_R[w(\infty)] &= 0 \end{aligned}\right\}. \tag{9}$$

The system of equations (6) was solved by a finite difference method, applied on a selected mesh

$$0 = \eta_O < \eta_1 \ldots < \eta_N \tag{10}$$

The boundary conditions $g_R[w(\infty)] = 0$ at $\eta = \infty$ were applied at a finite value of η_N; the solution was found to be insensitive to values $\eta_N \gtrsim 10$. The mesh points were selected so that the variation in the solution was approximately evenly distributed between them; in practice this meant that

$$\| w_i - w_{i-1} \| \lesssim \text{constant}$$

for each mesh interval. The introduction of this non-uniform mesh allowed the use of fewer mesh points for a given accuracy of solution [6].

The finite difference method was of the type discussed by Keller [7]. The trapezoidal rule, applied to the interval (η_{i-1}, η_i), gives

$$w_i - w_{i-1} - \frac{(\eta_i - \eta_{i-1})}{2}[F(w_i) + F(w_{i-1})] = 0. \tag{11}$$

Using this formulation for each interval, and applying the boundary conditions at η_O and η_N, gives a set of non-linear difference equations that are solved by a Newton method.

This numerical scheme, applied to the 1-dim. similarity equations, has easy conceptual extension to the 2-dim., parabolic equations of reacting flow. The

application of box schemes to parabolic equations was suggested, for example, by [8].

3. EXPERIMENTAL

3.1. *Location of transition to turbulent flow*

Values given in the literature [9] for the critical Grashof number for transition span the range of 10^8 to 8×10^9 and were all obtained at relatively small plate-to-ambient temperature differences. This previous information on transition from laminar to turbulent flow did not permit a reliable estimate of the transition point at the plate temperatures and surface-to-ambient temperature differences of interest in this study. The information was necessary, however, to determine the suitable experimental plate dimension.

A preliminary investigation of the boundary layer flow adjacent to a large, heated, polished, flat brass plate, 0.5 m high × 0.25 m wide × 0.00127 m thick was undertaken to determine the onset of transition at high plate-to-ambient temperature differences. An uncalibrated DISA hot wire probe was traversed along the length of the plate at a distance of ~ 1.5 mm from the surface. The output from this probe displayed the changes in local heat transfer at the wire surface. Hence, the onset of rapid fluctuations in temperature and velocity, which are characteristic of turbulence, could be detected. This was repeated for a series of plate temperatures.

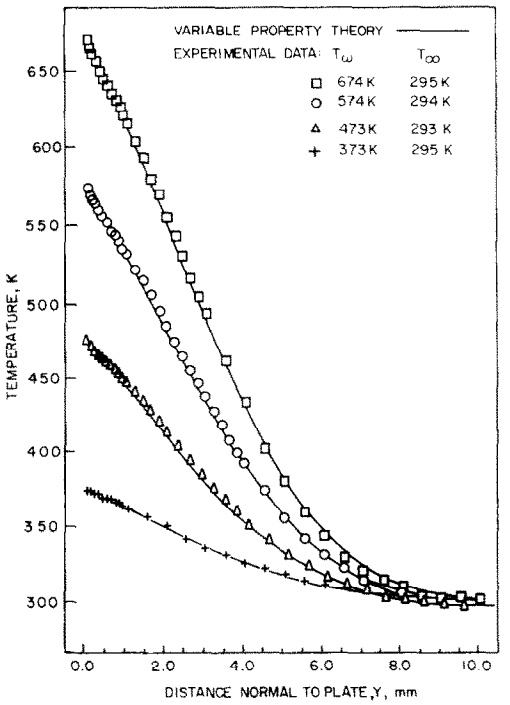

FIG. 1. Temperature profiles adjacent to a vertical isothermal hot plate — comparison of experimental and theoretical results ($x = 0.1$ m).

3.2. *Temperature profile measurement*

Temperature profiles were measured in the boundary layer flow adjacent to a small polished brass plate 0.114 m square. The plate was flush-mounted in a Sindanyo support and positioned in a stainless steel box which was open at the top and at the end facing the plate. A cooled leading edge section was fitted below the plate to prevent any starting length effect. A fine wire chromel–alumel thermocouple was used for the temperature measurement. The thermocouple junction (0.13 mm dia.) was supported horizontally and parallel to the plate by two thicker vertical support wires. This configuration minimised both conduction from the junction and interference of the upstream flow. Traverses of the boundary layer at one distance from the leading edge, $x = 0.1$ m, were carried out for a series of plate temperatures. Some instability was detected in the recorded temperature. This was caused by small disturbances within the room which could not be totally excluded. The probe signal was recorded for 2–3 min at each point and the average temperature recorded.

3.3. *Velocity profile measurement*

To overcome the problems of measuring low velocities in the difficult environment of the high thermal gradient that exists in the free convection boundary layer, we have applied the technique of real fringe laser Doppler anemometry to the measurement of the free convection velocity profiles. The laser anemometer system has been described in detail elsewhere [10]. The plate was that used for the temperature profile measurements. The stainless steel box was fitted with windows along the edge of the plate to permit optical access for the input beams. Collection of the scattered light was at right angles to the input beam, i.e. in the y direction. The crossover was aligned with a target on the vertical centre line of the plate at a known distance from the plate. The boundary layer was traversed from this reference point by traversing the whole anemometer assembly including the collection optics. Traverses of the boundary layer were carried out for several plate temperatures at distances of 0.05 and 0.1 m from the leading edge.

4. RESULTS AND DISCUSSION

The preliminary measurements using the large plate indicated that for surface temperatures 473 and 623 K turbulence was first observed at Grashof numbers of 4×10^8 and 3×10^8 respectively, where the fluid properties are evaluated at the bulk temperature. Obviously, these critical values will be altered considerably if we choose to evaluate the fluid properties at the film temperature or some suitable reference temperature. These values lie within the range quoted in [9] for transition at lower temperature differences. From a practical point of view, this experiment demonstrated that a maximum value of x for which laminar flow was stable under typical autoignition conditions was 0.2 m.

The temperature profile measurements for a range of plate temperatures are presented in Fig. 1, together

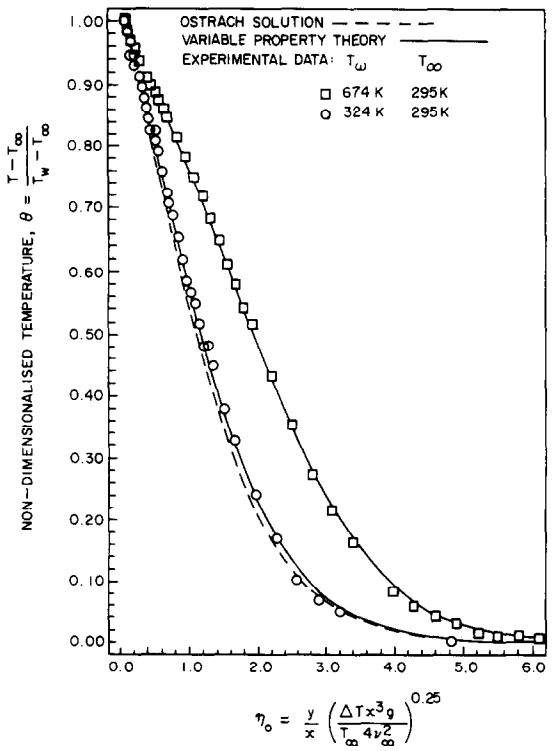

FIG. 2. Temperature profiles adjacent to a vertical isothermal hot plate—comparison of the variable fluid property model and the experimental results with Ostrach's solution ($x = 0.1$ m).

with the corresponding predictions from the model. The experimental and theoretical results show very good agreement for all the plate temperatures investigated. The experiments do, however, show a slightly greater inflection near the surface than is predicted by the model. The results for the highest and lowest temperatures investigated are presented (Fig. 2) using the non-dimensional variables θ and η_o and the bulk temperature as the reference condition. Ostrach's solution is shown for comparison using the same variables. This demonstrates very clearly that the constant property theory does not give an adequate representation of the temperature field at high plate-to-ambient temperature differences. For a small temperature difference (29 K) the constant property theory is a reasonable approximation, but the variable property solution is noticeably better.

Figure 3 compares the experimental data for the highest plate temperature with predictions using the Chapman–Rubesin approximation and three different values of M. The values of M correspond to the ambient temperature, the film temperature and the wall temperature. All three profiles are seen to be a significant improvement over the Ostrach solution (Fig. 2) indicating the importance of including the density variation in the definition of the similarity variable. The profile obtained using $M = 0.9$ (the film temperature value) gives a very close fit to the experimental results.

Table 1 presents the values obtained for wall heat transfer and shear stress, for these three values of M and for the full variable property model. By comparison with the full variable property model, the best values for these wall properties are obtained using the wall temperature value $M = 0.8$ in the Chapman–Rubesin approximation. It is thus seen that different values of M should be chosen when the Chapman–Rubesin approximation is used, depending upon whether heat transfer values or the overall fit of the temperature profile are more important.

The measured velocity profiles are presented in Fig. 4 in non-dimensional form. As the temperature difference between the plate and ambient increases the measured velocities deviate progressively from Ostrach's solution. This broadening of the boundary layer is described very well by the full variable property model as is the peak velocity. At the edge of the boundary layer particularly for the measurements made at $x = 0.1$ m the model does not agree very well with the experimental results. It is interesting to note that similar deviations from the theory have been observed in other experimental investigations [2, 11]. A recent experimental study [12] in which laser velocimetry was used for measurement of the velocity profiles adjacent to a vertical hot plate at 359 K gave results that agreed well with those of [2] but no data was presented for values of $\eta > 2.6$. At low Grashof numbers, the inadequacy of the first order boundary layer approximation could lead to this type of discrepancy between the model and experiment. However, the correction derived by [4] for 2nd-order effects does not account for the difference between experiment and theory for $\eta_o > 4$ (Fig. 5). The results are compared for the lowest plate temperature studied and the calculations were performed using the Chapman–Rubesin approximation with $M = 1$.

The discrepancy appears to be significantly greater for the measurements made at $x = 0.1$ m than at $x = 0.05$ m, indicating that it may be due to the proximity of the measurement point to the trailing edge. The experimental measurements were made just within the "trailing edge region" defined by [13] in their paper on the discussion of trailing edge effects. A rigorous attempt to treat the wake effects is probably not justified at this stage but it is shown in Fig. 5 that the simple corrections derived by [14] for wake effects make the agreement worse in the region near the edge of the boundary layer. We are thus forced to leave the question of the "tail" on the velocity profiles unexplained and we cannot rule out its existence being due to an undefined deficiency in the experimental system. Although our velocity measurements show clearly the improvement of the variable property theories over Ostrach's constant property theory they do not permit us to decide whether the higher order theories can give a significantly better representation of the flow under our conditions.

From the point of view of our declared objective, the study of chemically reacting flows, it is the hot zone

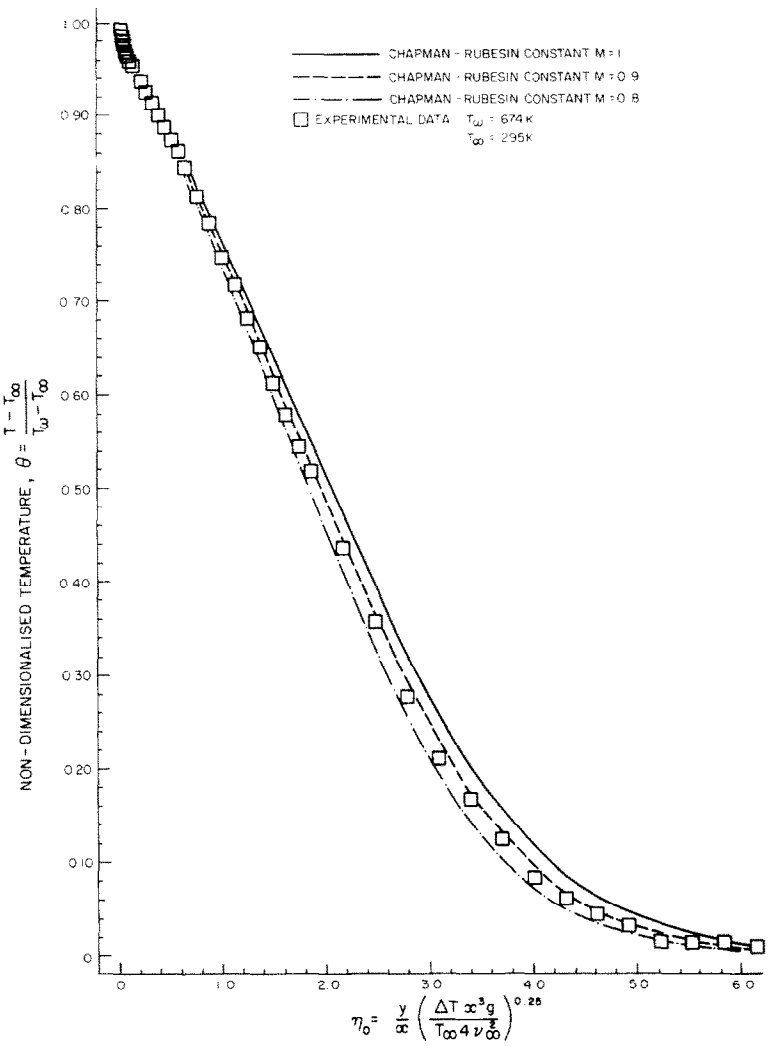

FIG. 3. Temperature profiles adjacent to a vertical isothermal hot plate. Comparison of a model using the Chapman–Rubesin approximation with the experimental results ($x = 0.1$ m).

Table 1. Comparison of wall flow properties (non-dimensional heat transfer and shear stress) predicted by the variable property model and by the Chapman–Rubesin model

Flow property	Variable property model	Chapman–Rubesin $M = M(T_x)$	Chapman–Rubesin $M = M(T_f)$	Chapman–Rubesin $M = M(T_w)$	T_w (K)	T_∞ (K)
$\frac{Nu_{x,w}}{\left(\frac{Gr_{x,x}}{4}\right)^{1/4}}$ (heat transfer)	0.565	0.502	0.529	0.561	674	294
$\frac{\mu_w\left(\frac{du}{dy}\right)_w}{\rho_w\left(\frac{\nu_w}{x}\right)^2}(Gr_{x,x})^{-3/4}\cdot\frac{\rho_r}{\rho_w}\cdot\frac{\nu_w}{\nu_r}$ (skin friction)	0.783	0.678	0.715	0.758	674	294

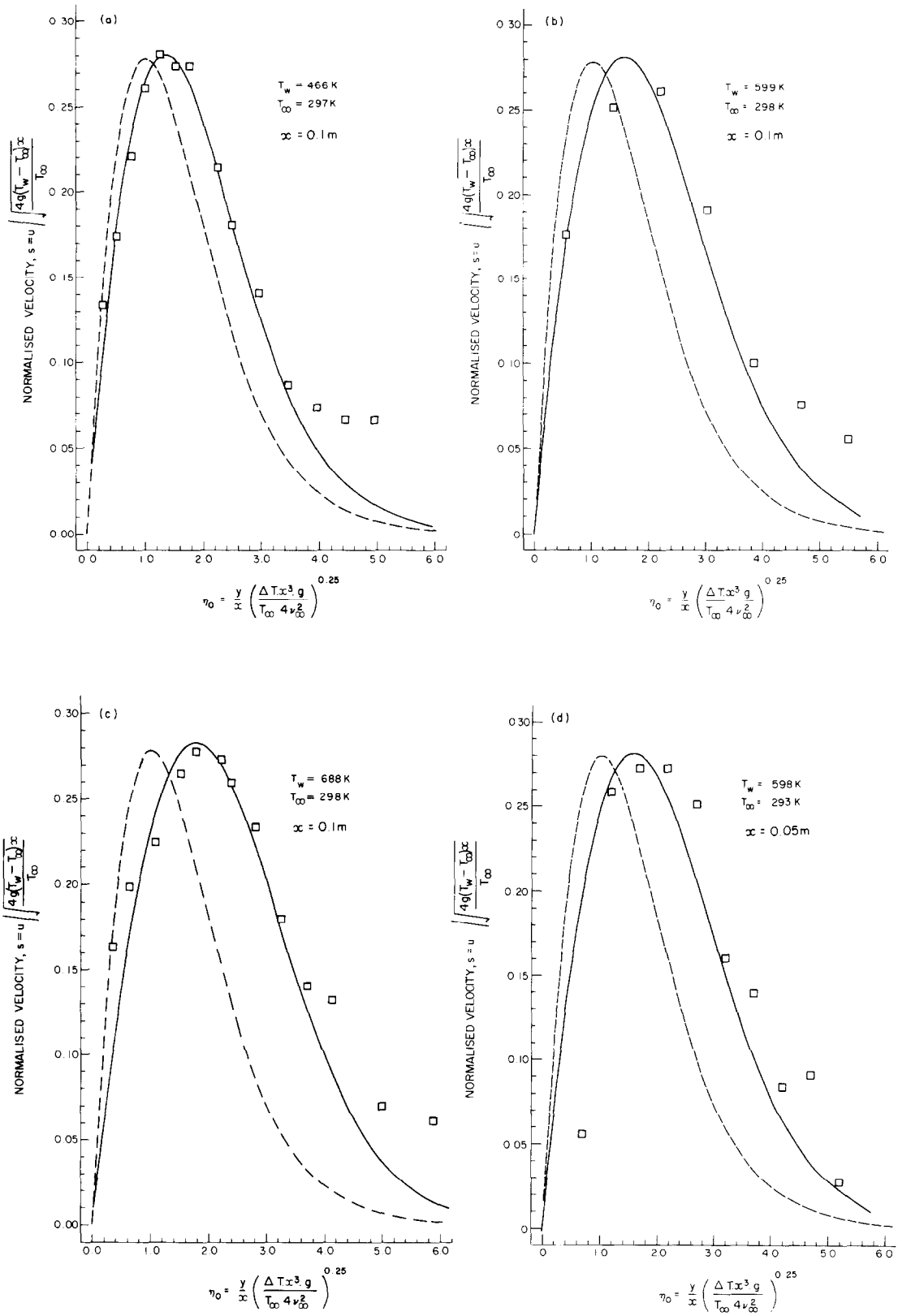

FIG. 4. Velocity profiles adjacent to a vertical isothermal hot plate — comparison of the experimental results with variable property model and with Ostrach's solution: ——— Ostrach's solution, ——— variable property theory, □ experimental data.

near the plate that is the region of interest. In this region, the variable property 1st-order theory gives an adequate representation of both the temperature and the velocity profiles; the Chapman–Rubesin approximation can also give a reasonable characterisation of the flow. Because of the simplification afforded by this approximation, particularly when extending calculations to include chemically reacting flows of mixtures of fluids, it will form the basis of our future work. The extension of the experimental technique and the numerical methods to the study of non-similar chemically reacting free convection boundary layers will be the subject of a future paper [15].

5. CONCLUSIONS

1. Experimental measurements of the velocity and temperature profiles in the free convection flow in air adjacent to very hot surfaces have been obtained using the techniques of laser Doppler anemometry and fine wire thermocouple thermometry.

2. Comparison of the experimental results with Ostrach's solution demonstrates quantitatively the limitations of the constant property approximation for free convection flows induced by large temperature differences.

3. A finite difference scheme, applied to the 1st-order formulation of the similarity equations, has been found to give accurate solutions for the boundary layer flow adjacent to a hot vertical plate. The inclusion of variable fluid properties was straightforward and comparison of the solutions with experimental results showed very good agreement.

4. Calculations of velocity and temperature profiles have been made using the Chapman–Rubesin approximation and a range of values of the representative constant. It has been shown that good agreement can

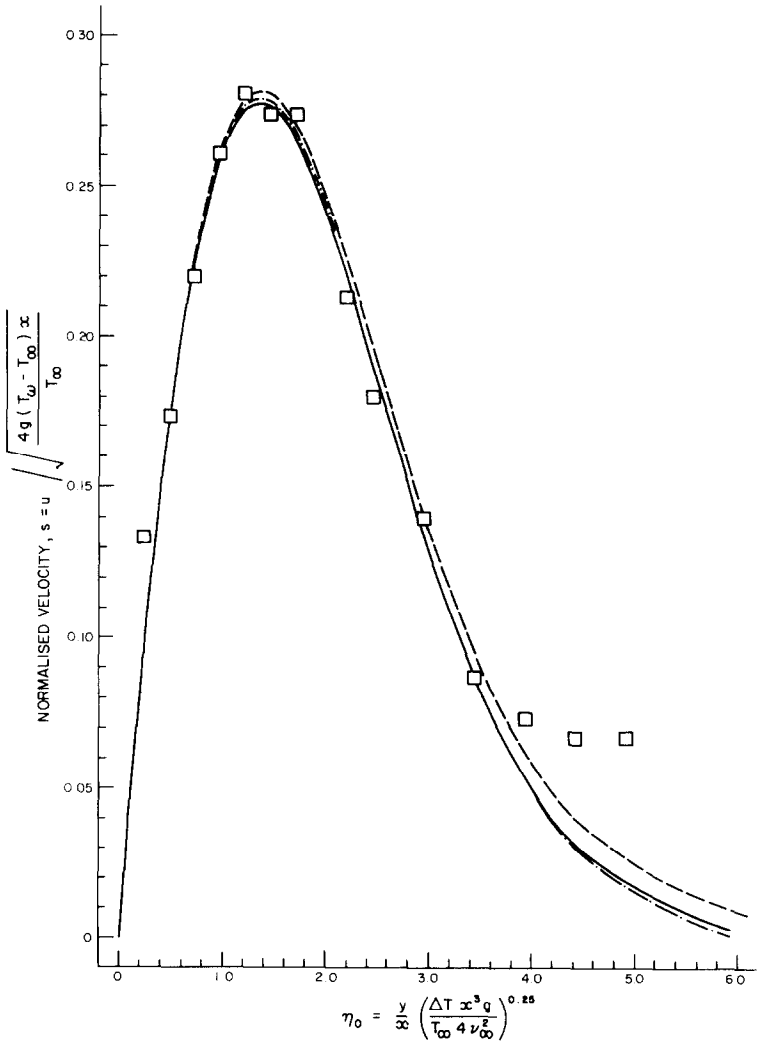

FIG. 5. Velocity profiles adjacent to a vertical hot plate: ——— variable property theory using Chapman–Rubesin approximation ($M = 1$), — — — same theory corrected for 2nd-order effects, — · — · — same theory corrected for 2nd-order and wake effects, □ experimental data ($T_w = 466$ K, $T_\infty = 297$ K, $x = 0.1$ m).

be obtained with this approach, although no single value of the constant will give good results for all the different characteristics of the flow.

5. The experimental and numerical techniques employed can later be used to investigate the progressive interaction between an exothermic chemical reaction and the convection temperature and velocity fields.

Acknowledgements—The authors wish to thank Drs J. B. Cole and M. D. Swords for the use of and assistance with the laser anemometer system, Mr P. A. Morgan and Dr G. Woodford for assistance with the experimentation and numerical analysis, respectively, and Dr D. C. Bull and Mr A. Prothero for critically reviewing the final manuscript.

REFERENCES

1. S. Ostrach, An analysis of laminar free convection flow and heat transfer about a flat plate parallel to the direction of the generating body force, NACA Technical Note 2635 (1952).
2. E. Schmidt and W. Beckmann, Das Temperatur und Geschwindigkeitsfeld vor einer Warme abegbenden senkrechten Platte bei naturlicher Konvektion, *Tech. Mech. Thermodyn.* **1**, 341 (1930).
3. E. M. Sparrow and J. L. Gregg, The variable fluid property problem in free convection, *Trans. ASME* 879 (1958).
4. J. F. Clarke, Transpiration and natural convection: the vertical-flat-plate problem, *J. Fluid Mech.* **57**, 45 (1973).
5. Y. R. Mayhew and G. F. C. Rogers, *Thermodynamic and Transport Properties of Fluids.* Oxford Univ. Press (1969).
6. C. E. Pearson, A numerical method for ordinary differential equations of boundary layer type, *J. Math. Phys.* **47**, 134–154 (1968).
7. H. B. Keller, Accurate difference methods for nonlinear two-point boundary value problems, *SIAM J. Num. Anal.* **11**, 305–320 (1974).
8. H. B. Keller, Numerical methods in boundary layer theory, *Ann. Rev. Fluid Mech.* **10**, 417–433 (1978).
9. F. Goudaux and B. Gebhart, An experimental study of the transition of natural convection flow adjacent to a vertical plate, *Int. J. Heat Mass Transfer* **17**, 93 (1974).
10. J. B. Cole and M. D. Swords, Laser Doppler anemometry measurements in an engine, *App. Optics* **18**, 1539 (1979).
11. R. Eichorn, Measurement of low speed gas flows by particle trajectories; a new determination of free convection velocity profiles, *Int. J. Heat Mass Transfer* **5**, 915 (1962).
12. R. D. Flack, Jr. and C. L. Wilt, Velocity measurements in two natural convection air flows using a laser velocimeter, *J. Heat Transfer* **101**, 256 (1979).
13. A. F. Messiter and A. Liñán, The vertical plate in laminar free convection: effects of leading and trailing edges and discontinuous temperature, *J. appl. Maths. Phys. (ZAMP)* **27**, 633 (1976).
14. K. T. Yang and E. W. Jerger, First order perturbations of laminar free convection boundary layers on a vertical plate, *J. Heat Transfer* **86**, 107 (1964).
15. L. R. Cairnie, A. J. Harrison and P. A. Morgan, Autoignition in a free convection boundary layer, *18th Symp. (Int.) on Combustion*, p. 1799. The Combustion Institute (1980).

CONVECTION NATURELLE ADJACENTE A UNE PLAQUE CHAUDE ISOTHERME ET VERTICALE AVEC UNE GRANDE DIFFERENCE DE TEMPERATURE PAR RAPPORT A L'AMBIANCE

Résumé—On étudie expérimentalement et théoriquement la convection naturelle de couche limite adjacente à une plaque chaude isotherme et verticale, avec une grande différence de température par rapport à l'ambiance. Des mesures expérimentales des champs de température et de vitesse, pour des températures de plaque allant jusqu'à 698 K, ont été faites en utilisant les techniques de la thermométrie par des thermocouples fins et de l'anémométrie laser Doppler. Les résultats expérimentaux s'écartent progressivement de la solution d'Ostrach quand la température de la plaque augmente. On obtient une solution numérique des équations de la couche limite qui inclut la dépendance vis-à-vis de la température des propriétés du fluide, dont la densité, en utilisant un schéma aux différences finies. On constate un très bon accord entre la solution numérique et les mesures expérimentales. Des calculs utilisant l'approximation de Chapman–Rubesin montrent que cette méthode donne une représentation adéquate de l'écoulement.

NATÜRLICHE KONVEKTION AN EINER SENKRECHTEN ISOTHERMEN HEISSEN PLATTE MIT GROSSER TEMPERATURDIFFERENZ ZWISCHEN PLATTENOBERFLÄCHE UND UMGEBUNG

Zusammenfassung—Die freie Konvektionsströmung an einer senkrechten isothermen heißen Platte mit großer Temperaturdifferenz zwischen Plattenoberfläche und Umgebung wurde experimentell und theoretisch untersucht. Messungen der Temperatur- und Geschwindigkeitsfelder für Plattenoberflächentemperaturen bis zu 698 K wurden mit Dünndraht-Thermoelementen bzw. Laser-Doppler-Anemometer durchgeführt. Die experimentellen Ergebnisse weichen mit steigender Plattentemperatur zunehmend von der Ostrach'schen Lösung ab. Eine numerische Lösung der Grenzschichtgleichungen, welche die Temperaturabhängigkeit der Fluideigenschaften einschließlich der Dichte enthält, wurde durch Anwerdung des finiten Differenzenverfahrens erhalten. Die numerische Lösung zeigte sehr gute Übereinstimmung mit den experimentellen Werten. Berechnungen mit der Chapman–Rubesin-Approximation haben gezeigt, daß diese Methode für viele Fälle eine angemessene Darstellung der Strömung ergibt.

ЕСТЕСТВЕННАЯ КОНВЕКЦИЯ У ВЕРТИКАЛЬНОЙ ИЗОТЕРМИЧЕСКОЙ НАГРЕТОЙ ПЛАСТИНЫ ПРИ БОЛЬШОЙ РАЗНИЦЕ ТЕМПЕРАТУР ПОВЕРХНОСТИ И ОКРУЖАЮЩЕЙ СРЕДЫ

Аннотация — Экспериментально и теоретически исследуется свободноконвективное течение около вертикальной изотермической нагретой пластины при большой разнице температур поверхности и окружающей среды. Экспериментальные измерения полей температуры и скорости при температурах пластины до 698 К производились соответственно термопарой и лазерным допплеровским анемометром. По мере увеличения температуры пластины экспериментальные данные начинают сильно отличаться от результатов, теоретически полученных Острачем. Конечно-разностным методом получено численное решение уравнений пограничного слоя с учетом температурной зависимости свойств жидкости, включая плотность. Получено хорошее совпадение результатов численного решения с экспериментальными данными. Расчеты на основании аппроксимации Чепмана Рубезина показали, что метод пригоден для описания различных течений.